RSC Advances




ROYAL SOCIETY OF CHEMISTRY

www.rsc.org/advances

Journal Name

ARTICLE

# Porphyrin Containing Lipophilic Amide Groups as Photosensitizer for Dye-sensitized Solar Cells

Received 00th January 20xx,
Accepted 00th January 20xx

DOI: 10.1039/x0xx00000x

www.rsc.org/

J. Gasiorowski,[a] N. Pootrakulchote,[b] C. Reanprayoon,[c] K. Jaisabuy,[d] P. Vanalabhpatana,[d] N. S. Sariciftci,[a] and P. Thamyongkit*[,d]

In this study, synthesis and investigation of a novel zinc-porphyrin derivative bearing $C_{24}$-containing amide groups for potential use in dye-sensitized solar cells (DSSCs) are presented. According to absorption spectra and electrochemical data, the target porphyrin has appropriate highest occupied molecular orbital (HOMO) and lowest unoccupied molecular orbital (LUMO) energy levels. The device studies revealed that the DSSCs based on the target porphyrin exhibited high light harvesting efficiency in the Q-bands region and the increased photocurrent, compared to the DSSCs based on benchmark derivative bearing no alkyl amide groups on the *meso*-phenyl substituents. The optimum DSSC based on the target porphyrin gave a short-circuit photocurrent density ($J_{sc}$), an open-circuit voltage ($V_{oc}$) and a fill factor (*FF*) of 5.6 mA·cm$^{-2}$, 0.7 V and 0.78, respectively, with the overall power conversion efficiency (PCE) of 3.1%.

## Introduction

With their large molar absorption coefficients, and amenability to structural modifications for tuning of the electrochemical and photophysical properties, porphyrin derivatives have attracted interest in the field of organic optoelectronics.[1] Since the great success in developing porphyrin-based dye-sensitized solar cells (DSSCs) with power conversion efficiency (PCE) of 12.3% in 2011,[2] intensive efforts have been put towards design and development of the novel porphyrins to enhance the cell efficiency. In the operation of the DSSCs, one of the critically undesirable pathways is charge recombination between photo-injected electron at $TiO_2$ and oxidized dye and/or electrolyte. Ballester and Palomares *et al.* reported the suppression of the recombination between photo-injected electron at $TiO_2$ and the electrolyte in the DSSCs by using of a porphyrin dye bearing $C_5$ alkyl groups on *meso*-phenyl substituents.[3] Moreover, the sizable linear alkyl chains were reported to form a hydrophobic layer covering the dye layer, resulting in higher stability of the DSSCs[4] and have the self-assembly property that can give the well-organized surface coverage of the dyes on the $TiO_2$ films and efficient electron injection.[5] In this work, we aim to synthesize and investigate a novel zinc-porphyrin bearing three $C_{24}$-containing amide groups, and a carboxyl group at para positions of the *meso*-phenyl substituents for its potential use in the DSSCs. The $C_{24}$ alkyl chain was used in this study as a representative of the long linear alkyl chains. An amide group was chosen to be a linker between the porphyrin macrocycle and the $C_{24}$ alkyl *meso*-substituents because it is known as a robust functional group that can be readily formed. Furthermore, the amide group was demonstrated to promote the self assembly in the dye layers of the organic solar cells by hydrogen bonding.[6] The photophysical and electrochemical properties of the target molecule, and the effect of the $C_{24}$-containing amide groups on the DSSC performance will give a useful guideline for the introduction of the long alkyl chains in the porphyrinic photosensitizing systems for the DSSCs.

## Experimental Section

**Material and Methods.** All chemicals were analytical grade, purchased from commercial suppliers and used as received without further purification. $^1$H-Nuclear magnetic resonance (NMR) and $^{13}$C-NMR spectra were obtained in deuterated chloroform ($CDCl_3$) using a NMR spectrometer operated at 400 megahertz (MHz) for $^1$H and 100 MHz for $^{13}$C nuclei. Chemical shifts (δ) are reported in parts per million (ppm) relative to the residual $CHCl_3$ peak (7.26 ppm for $^1$H-NMR and 77.0 ppm for $^{13}$C-NMR). Coupling constants (*J*) are reported in Hz. Mass spectra were obtained by matrix-assisted laser desorption ionization mass spectrometry (MALDI-MS) using dithranol as a matrix. Absorption and emission spectra of the solutions were measured in toluene at room temperature and an absorption extinction coefficient (ε) was reported in L/mol·cm. The absorption of the porphyrin film on $TiO_2$ was recorded at room temperature by using the same $TiO_2$ film as a blank.

[a.] Linz Institute for Organic Solar Cells (LIOS), Institute of Physical Chemistry, Johannes Kepler University of Linz, Linz 4040, Austria.
[b.] Department of Chemical Technology, Faculty of Science, Chulalongkorn University, Bangkok 10330, Thailand.
[c.] Program in Petrochemistry and Polymer Science, Faculty of Science, Chulalongkorn University, Bangkok 10330, Thailand.
[d.] Department of Chemistry, Faculty of Science, Chulalongkorn University, Bangkok 10330, Thailand. Fax: +662-254-1309; Tel: +662-218-7587; E-mail: patchanita.v@chula.ac.th

Electronic Supplementary Information (ESI) available: Spectral data, including $^1$H-NMR spectrum, $^{13}$C-NMR spectrum and mass spectra for new compounds. See DOI: 10.1039/x0xx00000x

**Non-commercial Compound.** Porphyrin **4** was prepared following literature procedure.[7]

**Synthesis of tetracosan-1-amine (3).** Following a published method[8] with modified reaction time and work-up procedure, a mixture of lignoceric acid (**1**, 1.002 g, 2.718 mmol) and thionyl chloride (1.800 g, 15.13 mmol) in tetrahydrofuran (THF, 4 mL) was refluxed for 1 h. The remaining thionyl chloride was removed under reduced pressure to obtain an orange brown oil containing tetracosanoyl chloride, which was treated with a cold aqueous ammonia solution (25% w/w, 20 mL) at room temperature. After 3 h, the mixture was extracted with $CH_2Cl_2$ (3 × 50 mL). The organic phase was collected and dried over anhydrous magnesium sulfate. After the removal of solvent under reduced pressure, the resulting yellow crude was treated with hexanes (30 mL). The mixture was then sonicated for 10 min and placed in a refrigerator (4 °C) overnight for precipitation. The resulting precipitate was filtered and washed with cold hexane and dried under vacuum to obtain tetracosanamide (**2**) as a colorless solid (0.802 g, 80%). $^1$H-NMR δ 0.87 (t, *J* = 6.8 Hz, 3H), 1.03–1.45 (m, 30H), 1.51–1.67 (m, 4H), 1.72–1.91 (m, 4H), 2.29 (t, *J* = 8.0 Hz, 2H), 3.53–3.60 (t, *J* = 6.4 Hz, 2H), 4.05–4.12 (t, *J* = 6.4 Hz, 2H); $^{13}$C-NMR δ 14.1, 22.7, 25.0, 26.1, 29.15, 29.18, 29.3, 29.4, 29.5, 29.6, 29.65, 29.69, 31.9, 34.3, 44.4, 63.3, 173.9; MALDI-TOF-MS m/z obsd 367.934 [$M^+$], calcd 367.652 (M = $C_{24}H_{49}NO$).

A solution of compound **2** (0.802 g, 2.18 mmol) in diethyl ether (20 mL) was treated with $LiAlH_4$ (0.805 g, 21.2 mmol) at 0 °C and the reaction was continued at room temperature for 17 h. After that, the reaction was quenched by adding water (1.00 mL), 15 % NaOH (1.00 mL) and then water (3.00 mL). The mixture was filtered and the resulting filtrate was concentrated under reduced pressure, leading to tetracosan-1-amine (**3**) as a colorless solid (0.515 g, 67%). $^1$H-NMR δ 0.82–0.97 (m, 11H), 1.00–1.49 (m, 18H), 1.49–1.63 (m, 8H), 1.63–1.77 (m, 2H), 1.77–1.96 (m, 2H), 2.67 (t, *J* = 6.8 Hz, 2H), 3.63 (m, 8H); $^{13}$C-NMR δ 14.1, 22.7, 25.8, 26.9, 29.35, 29.44, 29.5, 29.6, 29.7, 31.9, 32.8, 33.8, 42.2, 63.0; MALDI-TOF-MS m/z obsd 353.835 [$M^+$], calcd 353.668 (M = $C_{24}H_{51}N$).

**Synthesis of Zn-5.** Following a previously reported procdure[9] with modified stoichiometry, a solution of porphyrin **4**[7] (0.149 g, 0.188 mmol) in THF (10 mL) was treated with *N*-hydroxysuccinimide (NHS, 0.217 g, 1.88 mmol, 10 equiv.) and 1-ethyl-3-(3-dimethylaminopropyl)carbodiimide hydrochloride (EDC·HCl, 0.432 g, 2.26 mmol, 12 equiv.). The reaction mixture was stirred at reflux temperature for 2 d and then the solvent was removed under reduce pressure. The crude mixture was redissolved in THF (10 mL) and the resulting solution was treated with compound **3** (0.815 g, 2.30 mmol, 12 equiv.) and triethylamine (TEA, 5 mL). The reaction mixture was stirred at refluxing temperature for 1 d and then the solvent was removed under reduce pressure. Column chromatography [silica, $CH_2Cl_2$ : EtOH : TEA (96 : 3 : 1)] afforded a crude containing compound **5**: MALDI-TOF-MS m/z obsd 1800.122 [$M^+$], calcd 1797.733 (M = $C_{120}H_{177}N_7O_5$). Following a previously published procedure,[10] a solution of compound **5** in chloroform (3 mL) was reacted with a solution of zinc acetate dihydrate (0.045 g, 0.206 mmol) in methanol (1 mL) at room temperature for 3 h. After that, the resulting mixture was extracted by $CH_2Cl_2$ and $H_2O$. The organic phase was dried over anhydrous magnesium sulfate and concentrated under reduced pressure. The resulting solid was washed with hexane and then methanol to afford compound **Zn-5** as a purple solid (0.016 g, 5% from compound **4**). mp > 230°C (from methanol); $^1$H-NMR δ 0.81–0.92 (m, 12H), 1.15–1.59 (m, 81H), 1.68–1.83 (m, 6H), 1.85–2.60 (m, 30H), 3.36–3.78 (m, 18H), 6.43–6.51 (m, 3H), 8.09–8.18 (m, 6H), 8.20–8.30 (m, 8H), 8.40–8.52 (m, 2H), 8.74–8.87 (m, 8H); $^{13}$C-NMR δ 8.0, 8.1, 8.6, 11.1, 12.0, 14.0, 19.1, 22.6, 23.8, 25.5, 27.1, 27.7, 28.3, 28.6, 28.8, 29.0, 29.2, 29.4, 29.6, 29.8, 31.8, 39.6, 40.3, 42.2, 45.8, 52.9, 58.05, 58.09, 63.2, 65.2, 67.5, 67.9, 70.5, 119.2, 119.3, 120.2, 125.4, 127.[illegible] 131.3, 134.2, 134.4, 134.5, 141.2, 144.6, 144.8, 144.9, 167.4, 170.9; MALDI-TOF-MS m/z obsd 1862.492 [$M^+$], calcd 1861.127 (M = $ZnC_{120}H_{175}N_7O_5$); $\lambda_{abs}$ ($\varepsilon$) 426 (3.2 × $10^5$), 556, 597; $\lambda_{em}$ ($\lambda$ = 426 nm) 605, 651 nm.

**Electrochemical Studies.** Cyclic voltammetric measurements were carried out with an Autolab PGSTAT101 potentiostat/galvanostat (Eco Chemie, The Netherlands) using a conventional three-electrode configuration. A water-jacketed glass cell was employed to control the reaction temperature. A glassy carbon electrode with a disk diameter of 3.0 mm was used as a working electrode. Before use, the electrode was polished with an aqueous suspension of alumina powder and rinsed thoroughly with deionized water. A platinum wire was applied as an auxiliary electrode. All potentials are quoted with respect to a silver/silver ion ($Ag/Ag^+$) reference electrode in an acetonitrile solution; the electrode was externally calibrated with a ferrocene/ferrocenium ion ($Fc/Fc^+$) redox couple and has a potential of 0.548 V vs. normal hydrogen electrode (NHE).[11] Cyclic voltammograms were recorded at scan rates of 100–500 $mV\cdot s^{-1}$ in freshly distilled and deoxygenated $CH_2Cl_2$ containing 0.10 M tetrabutylammonium perchlorate (TBAP). A deaeration procedure was carried out with the aid of ultra-high purity (UHP) argon.

**Device Fabrication and Characterization.** A mesoscopic $TiO_2$ film composed of an 8-$\mu$m thick transparent layer of 20 nm sized $TiO_2$ anatase nanoparticles onto which a second 5 $\mu$m thick scattering layer of 400 nm sized $TiO_2$ was superimposed. The detailed methods for $TiO_2$ film preparation, device fabrication and photocurrent-voltage measurements can be found in the earlier report.[12] The double layer films were heated to 500 °C and sintered for 30 min. After cooling down to 80 °C, the film were immersed into the dye solution (300 $\mu$M) in a mixture of THF and ethyl alcohol (v/v, 1/4) for 16 h. The stained photoanode was fabricated with the platinized counter electrode using a 25 $\mu$m thick Surlyn film (Dupont, USA) and sealed by a hot-press machine. In this study, an acetonitrile based electrolyte containing 1.0 M 1,3-dimethylimidazolium iodide (DMII), 0.1 M LiI, 30 mM $I_2$, 0.5 M *tert*-butylpyridine

(tBP), and 0.1 M guanidiniumthiocyanate (GNCS) in a mixed solvent of acetonitrile and valeronitrile (v/v, 85/15) was used to fill the internal gap between two glasses.

To characterize the solar cells, a 450 W xenon light source (Oriel, USA) was used. The current-voltage characteristics were obtained by applying external potential bias to the cell and measuring the generated photocurrent with a Keithley model 2400 digital source meter (Keithley, USA). The devices were masked to attain an illuminated active area of 0.159 $cm^2$. Loss of light reflection from photoanode glass was reduced by applying a self-adhesive fluorinated polymer anti-reflecting film (ARKTOP, Asahi glass). Up to four devices were fabricated for each experimental variable change to make the opportune statistics. A modulated light intensity data acquisition system was used to control the incident photon-to-current conversion efficiency (IPCE) measurement. The modulation frequency was about 1 Hz. Light from a 300 W Xenon lamp (ILC Technology, USA) was focused through a computer controlled Gemini-180 double monochromator (JobinYvon Ltd., UK) onto the photovoltaic cell. White light bias was used to bring the total light intensity on the device closer to operating conditions.

Photovoltage transients were detected by using a pump pulse generated by four red light emitting diodes controlled by a fast solid-state switch with the white light bias. The pulse of the red light with the width of 50 ms was incident on the photoanode side of the cell, and its intensity was controlled to keep a suitably low level to generate the exponential voltage decay where the charge recombination rate constants were obtained directly from the exponential decay rate.[13] The white bias light, also incident on the same side of the devices, was supplied by white diodes. The photo-induced charge density as function of the white light bias intensity was obtained by charge extraction measurement where the stored charges under open circuit conditions were extracted by placing the cell under short circuit conditions.

## Results and Discussion

**Synthesis.**

The synthesis started with the reaction between lignoceric acid (**1**) and thionyl chloride to obtain the corresponding acid chloride, which was reacted further with a 25% $NH_4OH$ solution, leading to compound **2** in 80% yield (Scheme 1). After that, compound **2** was reduced by $LiAlH_4$ to afford compound **3** in 67% yield.

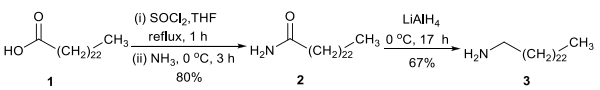


**Scheme 1.** Synthesis of amine precursor **3**

The preparation of the target compound relies on a three-step procedure recently published by our group.[9] Compound **4**[7] was subjected to a reaction of with NHS and EDC·HCl, followed by a condensation of the resulting air-sensitive succinimidyl ester with an excess amount of amine **3** to give freebase porphyrin **5** (Scheme 2). The yields from these two steps were low mainly due to the incompletion of the reaction at three reaction sites as desired, although the large excess of NHS, EDC·HCl and amine **3**, and the long reaction time were used. Moreover, attempts to separate compound **5** from other possible condensed by-products and impurities failed give pure compound **5**. Therefore, the resulting crude containing **5** was directly metallated by $Zn(OAc)\cdot 2H_2O$. After the lengthy chromatographic separation, **Zn-5** was obtained in 5% overall yield. In a mass spectrum, a molecular ion peak of **Zn-5** was observed at m/z 1862.492, confirming the formation of **Zn-5**. The solubility of **Zn-5** in common organic solvents, *e.g.* $CH_2Cl_2$, $CHCl_3$, and THF, was found to be approximately 10 $mg\cdot mL^{-1}$, which is sufficient for a routine wet process in the DSSC fabrication.

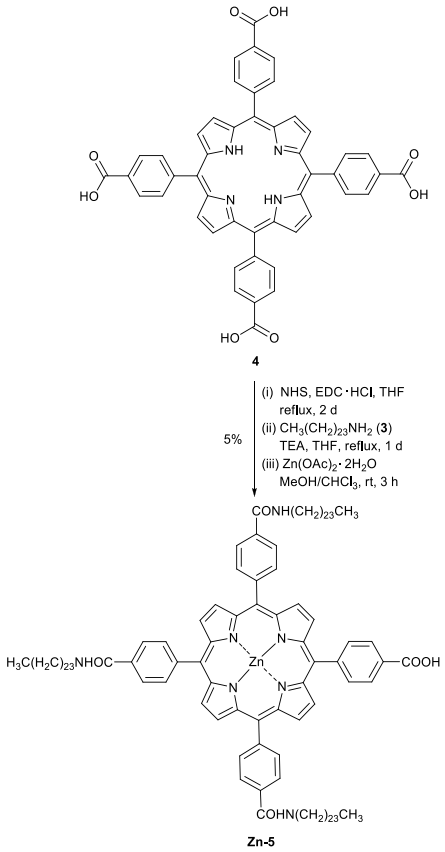


**Scheme 2.** Synthesis of the target compound

**Photophysical and Electrochemical Properties.**

As shown in Figure 1, an absorption spectrum of a **Zn-5** solution in toluene exhibited a characteristic pattern of Zn-porphyrin having an intense B-band at 426 nm, and Q-bands at 556 and 597 nm (black solid line). The absorption pattern of a **Zn-5** film on $TiO_2$ was very similar with slightly broader bands than those of the **Zn-5** solution, most likely due to the aggregation of the porphyrin macrocycle (red dashed line). This observation indicated that the $C_{24}$-containing amide

groups on the *meso*-phenyl substituents of the porphyrin ring did not significantly affect the photophysical properties of **Zn-5** in terms of absorption as a function of the wavelength of an incident light.

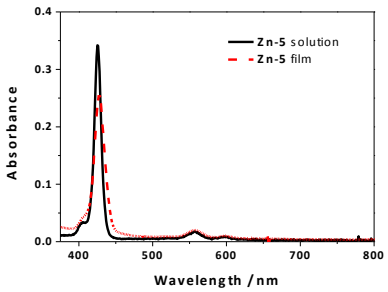


**Figure 1.** Absorption spectra of the **Zn-5** solution in toluene (black solid line) and the **Zn-5** film on $TiO_2$ (red dashed line)

Shown in Figure 2 are cyclic voltammograms obtained with a glassy carbon electrode at the scan rate of 100 mV·s$^{-1}$ in the potential range of –2.20 to 1.40 V for $CH_2Cl_2$ containing 0.10 M TBAP in the presence and absence of 1.00 mM **Zn-5**. Curves B and D, recorded as background cyclic voltammograms, exhibit no significant peaks of the TBAP-$CH_2Cl_2$ electrolyte solution. In the positive potential region, a cyclic voltammogram for the oxidation of **Zn-5** (curve A) reveals some electrochemical features of **Zn-5**. As fairly seen in the inset of Figure 2 presenting the magnified voltammograms from 0.30 to 1.30 V, three successive quasireversible redox couples exist. The anodic peak potentials are approximately at 0.54, 0.79 and 1.01 V, while the corresponding cathodic peak potentials are at 0.46, 0.71 and 0.92 V, respectively. When the potential was negatively scanned from 0 V to –2.20 V (curve C), the electro-reduction of **Zn-5** gave relatively small and poorly-defined irreversible cathodic peaks approximately at –0.81, –1.13, –1.33, –1.61, –1.91 and –2.08 V, implying multi-step ligand-centered reduction of porphyrinic units and the conjugated system of the compound.[14]

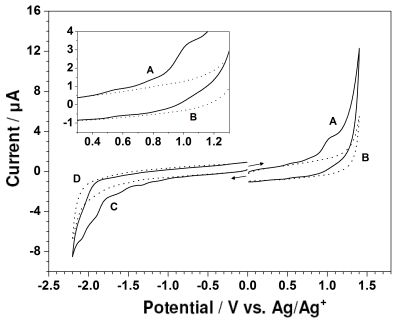


**Figure 2.** Cyclic voltammograms recorded with the glassy carbon electrode (area = 0.071 cm$^2$) at 100 mV·s$^{-1}$ in $CH_2Cl_2$ containing 0.10 M TBAP in the presence of 1.00 mM **Zn-5** (curves A and C) and $CH_2Cl_2$ containing only 0.10 M TBAP (curves B and D). Curves A and B were initially scanned in the positive direction; while curves C and D were initially scanned in the negative direction. Inset is an expansion of the region between 0.30 and 1.30 V.

To enhance the current size and thoroughly observe the electrochemical behavior of **Zn-5**, its cyclic voltammograms were further collected at the scan rates of 250 and 500 mV·s$^{-1}$. Figures 3a and 3b display cyclic voltammograms of 1.00 mM **Zn-5** solution initially scanned in anodic and cathodic directions, respectively, at 100, 250 and 500 mV·s$^{-1}$. All peaks appearing in the cyclic voltammograms recorded at 100 mV·s$^{-1}$ also exist in those collected at the higher scan rates with larger magnitudes and slight shifts in position. Table 1 summarizes peak potential ($E_p$) for the oxidation and reduction of **Zn-5** at these three scan rates. Due to the inexplicitness of some peaks especially those of reduction processes, each cyclic voltammetric peak was treated as a parabolic curve of which vertex represents the peak potential. Using scientific graphing and data analysis software, two tangent lines from both sides were drawn to achieve the intercept which is connected with the vertex via a straight line perpendicular to the parabolic base.[15] To achieve accurate peak potential values, at least three measurements were made at all positions and the relative standard deviations of the obtained potentials are less than 0.35%.

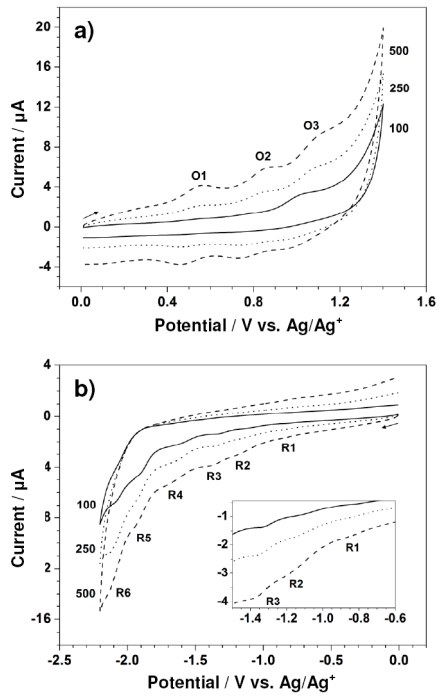


**Figure 3.** Cyclic voltammograms recorded with the glassy carbon electrode (area = 0.071 cm$^2$) from (a) 0 to +1.40 to 0 V and (b) 0 to –2.20 to 0 V in $CH_2Cl_2$ containing 0.10 M TBAP and 1.00 mM **Zn-5** at 100 (solid line), 250 (dotted line), and 500 (dashed line) mV·s$^{-1}$. Inset is an expansion of the region between –0.60 and –1.50 V.

For the oxidation of **Zn-5**, the differences between the anodic and cathodic peak potentials ($\Delta E_p$) of the three redox couples are approximately 80–110 mV. Since an electron transfer in high-resistance organic media always gives $\Delta E_p$ larger than the theoretical value of 59/n mV[16] and $\Delta E_p$ for the one-electron reversible $Fc/Fc^+$ couple in the 0.10 M TBAP-$CH_2Cl_2$ solution

Journal Name

ARTICLE

**Table 1**. Peak potential ($E_p$) values for the cyclic voltammograms of **Zn-5**

| Scan rate / mV·s$^{-1}$ | Oxidation (from 0 to 1.40 to 0 V) | | | | | | Reduction (from 0 to −2.20 to 0 V) | | | | | |
|---|---|---|---|---|---|---|---|---|---|---|---|---|
| | $E_{pa}$ in the forward scan / V | | | $E_{pc}$ in the backward scan / V | | | $E_{pc}$ in the forward scan / V | | | | | |
| | O1 | O2 | O3 | O1 | O2 | O3 | R1 | R2 | R3 | R4 | R5 | R6 |
| 100 | 0.54 | 0.79 | 1.01 | 0.46 | 0.71 | 0.92 | −0.81 | −1.13 | −1.33 | −1.61 | −1.91 | −2.08 |
| 250 | 0.55 | 0.84 | 1.07 | 0.46 | 0.74 | 0.97 | −0.82 | −1.17 | −1.36 | −1.67 | −1.92 | −2.09 |
| 500 | 0.55 | 0.84 | 1.07 | 0.46 | 0.74 | 0.97 | −0.84 | −1.17 | −1.37 | −1.67 | −1.92 | −2.12 |

$E_{pa}$= anodic peak potential; and $E_{pc}$ = cathodic peak potential.
Each entry represents the average peak potential value achieved from at least three measurements.
The potential is quoted with respect to the Ag/Ag$^+$ reference electrode and externally calibrated with the Fc/Fc$^+$ redox couple having a potential of 0.548 V vs. NHE.[11]

has a value of nearly 120 mV (data not shown), each oxidation of **Zn-5** in $CH_2Cl_2$ is possibly involved with one electron. In addition, it is worthwhile to consider the effect of the scan rate on peak current even though not all of the peak currents could be determined due to size limitation. For the third oxidation (O3), the anodic peak currents at 100, 250 and 500 mV·s$^{-1}$ are 1.41, 2.05 and 3.01 μA, respectively. A plot of these anodic peak currents vs. square root of scan rates demonstrates linear behavior (not shown), elucidating the diffusion-controlled oxidation process of **Zn-5**.

Using the data in Table 1, half-peak potential ($E_{1/2}$) for the oxidation of **Zn-15** in $CH_2Cl_2$ containing 0.10 M TBAP can be calculated. Table 2 displays $E_{1/2}$ values of all three oxidation. Following the previous studies,[17] the data from cyclic voltammetry and absorption spectroscopy can be used to estimate a highest occupied molecular orbital (HOMO) and lowest unoccupied molecular orbital (LUMO) energy level of the dyes. The $E_{1/2}$ value of the first oxidation ($E_{1/2}$(ox1)) can represent the HOMO energy level of a dye, while the LUMO one can be calculated from an excited state oxidation potential ($E_{0\text{-}0}^*$) by a following equation:

$E_{0\text{-}0}^* = E_{1/2}(\text{ox1}) - E_{0\text{-}0}$,

when $E_{0\text{-}0}$ is the absorption onset of the dye that represents its energy gap. The results indicated that the HOMO energy level and the energy gap of **Zn-5** were +0.50 V and 2.03 V, respectively. Therefore, its LUMO energy level was calculated to be −1.53 V. With the LUMO energy level being more negative than the conduction band of $TiO_2$ (−0.50 V vs. NHE[17]), the electron injection of the excited dye to $TiO_2$ surface should be thermodynamically possible in the **Zn-5**-based DSSCs. At the same time, the more positive energy level of its HOMO compared with the oxidation potential of an iodide ion/triiodide ion ($I^-/I_3^-$) redox couple (+0.40 V vs. NHE[17]) suggested that the dye regeneration by the $I^-/I_3^-$ electrolyte should be also favorable in the devices.

**Table 2**. Half-peak potential ($E_{1/2}$) values for the oxidation of **Zn-5**

| Scan rate / mV·s$^{-1}$ | Half-peak potential ($E_{1/2}$) / V | | |
|---|---|---|---|
| | O1 | O2 | O3 |
| 100 | 0.50 | 0.75 | 0.97 |
| 250 | 0.51 | 0.79 | 1.02 |
| 500 | 0.51 | 0.79 | 1.02 |

$E_{1/2}$ = ($E_{pa}$ + $E_{pc}$)/2, when $E_{pa}$ = anodic peak potential and $E_{pc}$ = cathodic peak potential.[16]
The potential is quoted with respect to the Ag/Ag$^+$ reference electrode and externally calibrated with the Fc/Fc$^+$ redox couple having a potential of 0.548 V vs. NHE.[11]

**Photovoltaic Characteristics.**

The photovoltaic performance of **Zn-5**-based DSSCs, *i.e.* the photocurrent density-voltage (*J-V*) curve and IPCE was investigated in test devices using a standard double layer $TiO_2$ film (8+5 μm) and a volatile acetonitrile-based electrolyte. The detailed composition is described in the device fabrication section. The IPCE of **Zn-5**-based device in Figure 4 shows the peak values of 49.1%, 35.2% and 30.7% at 440, 560 nm and 610 nm, respectively. These IPCE peaks are in accordance with the respective B-band and Q-bands in the absorption spectrum of **Zn-5** in the solution shown in Figure 1. It can be implied from the IPCE spectrum that the ratio of the peaks of the low-energy photon absorption to the peak of the high-energy photon absorption appeared to be 0.72 and 0.63 at the respective wavelength of 570 and 610 nm. These values are almost two times higher than those obtained from IPCE data of **ZnTPP-COOH** (approximately 0.3 and 0.2).[18] This suggested a substantial enhancement in the light harvesting efficiency in the visible region of **Zn-5** absorbed on the $TiO_2$ surface as result of the $C_{24}$-containing amide groups on the *meso*-phenyl substituents of the porphyrin macrocycle.

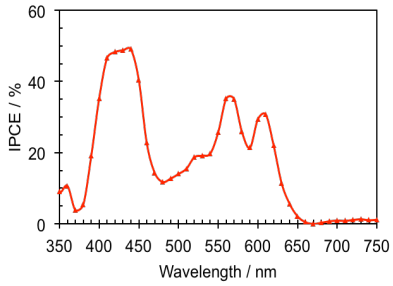


**Figure 4.** IPCE spectrum of the **Zn-5**-based DSSCs

The *J-V* curves of the devices with the volatile electrolyte under standard light illumination (AM 1.5 G 100 mW·cm$^{-2}$) are shown in Figure 5. The best **Zn-5**-based DSSC exhibited photovoltaic parameters; *i.e.* short-circuit photocurrent density ($J_{sc}$), an open-circuit voltage ($V_{oc}$) and a fill factor (*FF*) of 5.6 mA·cm$^{-2}$, 0.7 V and 0.78, respectively, which yielded a photoconversion efficiency (*PCE*) of 3.1%. To our surprise, the $J_{sc}$ of the device has been increased up to 180% of the original value by simply exposing the device under the simulated full sunlight for 40 minutes before the *J-V* measurement, leading to the increment of the PCE value from 1.6% to 3.1%. We assume that the steric effect of porphyrin bearing the $C_{24}$-containing amide groups can be subdued by the light exposure, allowing more photoelectrons to be generated and raising a passage of electrons throughout the redox mediator. On the other hand, by comparing with the results observed from **ZnTPP-COOH** that was reported earlier,[18] it was found that the presence of the $C_{24}$-containing amide groups at para positions of the *meso*-phenyl substituents of **Zn-5** caused remarkable increase in the photocurrent (4.2 vs. 5.6 mA·cm$^{-2}$). This phenomenon can be attributed to the long alkyl moieties enfolding in the circumference of the porphyrin macrocycles which decelerate the rate of charge recombination between the photo-injected electron and $I_3^-$ ions in the electrolyte at the $TiO_2$/electrolyte interface, corresponding to the previous studies.[3] Nevertheless, the measured PCEs of the **Zn-5** based devices are relatively low. This might be resulted from the low amount of surface coverage of the dye molecules on $TiO_2$ film due to the bulkiness of the long alkyl groups and the porphyrin aggregation on the $TiO_2$ surface that was also found in the preceding reports.[3,5,18]

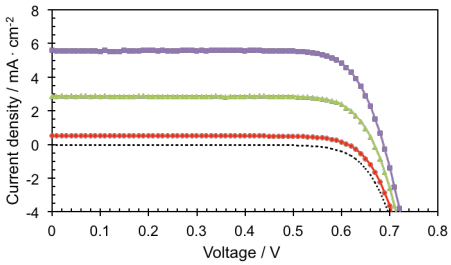


**Figure 5.** Photocurrent density-voltage curves of the **Zn-5**-based DSSCs

In order to elucidate the rate of electron recombination between **Zn-5**, $TiO_2$ nanoparticles and the oxidized electrolyte, the transient photovoltage decay measurement was performed. Figure 6a shows the electron recombination lifetime, which is the inverse of the recombination rate of the injected electrons, as a function of $V_{oc}$ in the device. This data represents the difference between the redox level of the electrolyte and the quasi-Fermi level in the $TiO_2$.[19] It appears in this plot that the electron lifetime decays exponentially with the stronger light intensity, suggesting that the recombination processes of the photoelectrons occur faster via the $I_3^-$ ions in the electrolyte, compared with the recombination processes via the $TiO_2$ phase, when the photoelectrons are filled in the higher energy states of $TiO_2$. In addition, Figure 6b shows the chemical capacitance-voltage characteristics of the device. The chemical capacitance is a representation of the electron density of state that increases with bias potential at open circuit condition as the density of state occupancy progresses. It is implied from Figure 6b that the chemical capacitance dependence on $V_{oc}$ exhibits an approximate exponential form

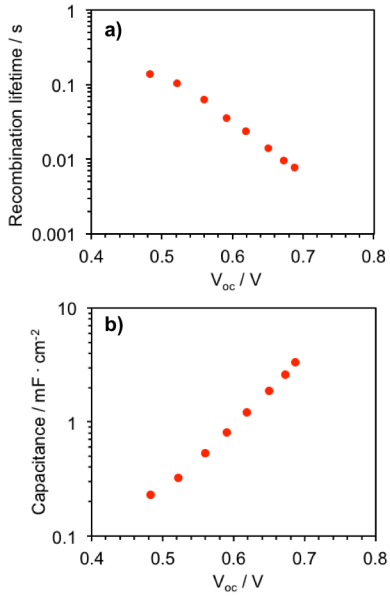


**Figure 6.** (a) Electron recombination lifetime and (b) chemical capacitance plotted as a function of open circuit voltage in the **Zn-5**-based DSSCs, derived from photovoltage transients at the various white light bias intensities

## Conclusions

This study has shown that synthesis of the target porphyrin bearing three $C_{24}$-containing amide groups and a carboxyl group on *meso*-phenyl substituents was achieved. The presence of the $C_{24}$-containing amide groups did not significantly affect the photophysical properties of the porphyrin dye. Cyclic voltammetry measurement gave good understanding on the electrochemical behaviour of the dye and also indicated that the HOMO-LUMO energy levels were suitable of the dye for DSSC application. The device studies indicated that the presence of the $C_{24}$-containing amide groups led to significant improvement of the DSSCs in terms of more efficient light harvesting in the Q-bands region and higher photocurrent, compared to the previously reported **ZnTPP-COOH**-based DSSCs.

## Acknowledgements

This research was supported by National Research University Project of Thailand, Office of the Higher Education Commission (Project No: WCU-035-EN-57), and Graduate School of Chulalongkorn University (The 90th Anniversary of Chulalongkorn University Fund, Ratchadaphiseksomphot Endowment Fund). The device fabrications and the photovoltaic measurements were performed at École Polytechnique Fédérale de Lausanne (EPFL), Switzerland.

## References

1 Selected publications: (a) K. Kalyanasundaram, N. Vlachopoulos, V. Krishnan, A. Monnier and M. Grätzel, *J. Phys. Chem.*, 1987, **91**, 2342. (b) A. Kay and M. Grätzel, *J. Phys. Chem.*, 1993, **97**, 6272. (c) D. Wohrle, B. Tennigkeit, J. Elbe, L. Kreienhoopand G. Schurpfeil, *Mol. Cryst. Liq. Cryst.*, 1993, **230**, 221. (d) S. Cherian and C. C. Wamser, *J. Phys. Chem. B*, 2000, **104**, 3624. (e) F. Odobel, E. Blart, M. Lagree, M. Villieras, H. Boujtita, N. El Murr, S. Caramori and C. A. Bignozzi, *J. Mater. Chem.*, 2003, **13**, 502. (f) W. M. Campbell, A. K. Burrell, D. L. Officer and K. W. Jolly, *Coord. Chem. Rev.*, 2004, **248**, 1363. (g) H. Imahori, *J. Phys. Chem. B*, 2004, **108**, 6130. (h) T. Hasobe, S. Fukuzumi and P. V. Kamat, *J. Phys. Chem. B*, 2006, **110**, 25477. (i) M. A. Baldo, D. F. O'Brien, Y. You, A. Shoustikov, S. Sibley, M. E. Thompson and S. R. Forrest, *Nature*, 1998, **395**, 151. (j) R. C. Kwong, S. Sibley, T. Dubovoy, M. Baldo, S. R. Forrest and M. E. Thompson, *Chem. Mater.*, 1999, **11**, 3709. (k) T. F. Guo, S. C. Chang, Y. Yang, R. C. Kwong and W. E. Thompson, *Org. Electrochem.*, 2000, **1**, 15. (l) E. M. Gross, N. R. Armstrong and R. M. Wightman, *J. Electrochem. Soc.*, 2002, **149**, E137. (m) V. A. Montes, C. Perez-Bolivar, N. Agarwal, J. Shinarand P. Anzenbacher, *J. Am. Chem. Soc.*, 2006, **128**, 12436. (n) X. Wang, H. Wang, Y. Yang, Y. He, L. Zhang, Y. Li and X. Li, *Macromolecules*, 2010, **43**, 709. (o) Y. Y. Noh, K. Yase, S. Nagamatsu, *Appl. Phys. Lett.*, 2003, **83**, 1243. (p) P. Checcoli, G. Conte, S. Salvatori, R. Paolesse, A. Bolognesi, A. Berliocchi, F. Brunetti, A. D'Amico, A. Di Carlo and P. Lugli, *Synth. Met.*, 2003, **138***,* 261. (q) P. B. Shea, J. Kanicki and N. Ono, *J. Appl. Phys.*, 2005, **98**, 014503. (r) C.-M. Che, H.-F. Xiang, S. S.-Y. Chui, Z.-X. Xu, V. A. L. Roy, J. J. Yan, W.-F. Fu, P. T. Lai and I. D. Williams, *Chem. Asian J.*, 2008, **3**, 1092.

2 (a) A. Yella, H.-W. Lee, H. N. Tsao, C. Yi, A. K. Chandiran, M. K. Nazeeruddin, E. W.-G. Diau, S. M. Zakeeruddin and M. Grätzel, *Science*, 2011, **334**, 629. (b) S. Mathew, A. Yella, P. Gao, R. Humphry-Baker, B. F. E. Curchod, N. Ashari-Astani, I. Tavernelli, U. Rothlisberger, M. K. Nazeeruddin and M. Grätzel, *Nature Chem.*, 2014, **6**, 242.

3 (a) A. Forneli, M. Planells, M. A. Sarmentero, E. Martinez-Ferrero, B. C. O'Regan, P. Ballester and E. Palomares, *J. Mater. Chem.*, 2008, **18**, 1652. (b) M. Planells, A. Forneli, E. Martinez-Ferrero, A. Sánchez-Díaz, M. A. Sarmentero, P. Ballester, E. Palomares and B. C. O'Regan, *Appl. Phys. Lett.*, 2008, **92**, 153506.

4 J. E. Kroeze, N. Hirata, S. Koops, M. K. Nazeeruddin, L. Schmidt-Mende, M. Grätzel and J. R. Durrant, *J. Am. Chem. Soc.*, 2006, **128**, 16376.

5 A. Islam, S. P. Singh, M. Yanagida, M. R. Karim and L. Han, *Int. J. Photoenergy*, 2011, **2011**, 757421.

6 (a) Z. Xiao, K. Sun, J. Subbiah, S. Ji, D. J. Jones and W. W. H. Wong, *Sci. Rep.*, 2014, **4**, 5701. (b) T. Aytun, L. Barreda, A. Ruiz-Carretero, J. A. Lehrman and S. I. Stupp, *Chem. Mater.*, 2015, **7**, 1201.

7 A. D. Adler, F. R. Longo, J. D. Finarelli, J. Goldmacher, J. Assour and L. Korsakoff, *J. Org. Chem.*, 1967, **32**, 476.

8 N. M. Howarth, W. E. Lindsell, E. Murray and P. N. Preston, *Tetrahedron*, 2005, **61**, 8875.

9 C. Reanprayoon, J. Gasiorowski, M. Sukwattanasinitt, N. S. Sariciftci and P. Thamyongkit, *RSC Adv.*, 2014*,* **4**, 3045.

10 J. Jiao, P. Thamyongkit, I. Schmidt, J. S. Lindsey and D. F. Bocian, *J. Phys. Chem. C*, 2007, **111**, 12693.

11 V. V. Pavlishchuk and A.W.Addison, *Inorg. Chim. Acta*, 2000, **298**, 97.

12 P. Wang, M. Zakeeruddin, P. Comte, R. Charvet, R. Humphry-Baker and M. J. Graetzel, *Phys. Chem. B,* 2003, **107,** 14336.

13 B. C. O'Regan and F. Lenzmann, *J. Phys. Chem. B*, 2004, **108**, 4342.

14 M. E. El-Khouly, J. B. Ryu, K.-Y. Kay, O. Ito and S. Fukuzumi, *J. Phys. Chem. C,* 2009, **113,** 15444.

15 Selected publications: (a) J. L. Coolidge, *Am. Math. Mon.*, 1951, **58,** 449. (b) P. R. Wolfson, *Am. Math. Mon.*, 2001, **108**, 206. (c) J. Stewart, Single Variable Calculus, 7th ed., Brooks/Cole Cengage Learning, USA 2008.

16 A. J. Bard and L. R. Faulkner, Electrochemical Methods: Funda-mentals and Applications, 2nd ed., Wiley, New York, 2000.

17 (a) S.-L. Wu, H.-P. Lu, H.-T. Yu, S.-H. Chuang, C.-L. Chiu, C.-W. Lee, E. W.-G. Diau and C.-Y. Yeh, *Energy Environ. Sci.*, 2010, **3**, 949. (b) A. Luechai, N. Pootrakulchote, T. Kengthanomma, P. Vanalabhpatana and P. Thamyongkit, *J. Organomet. Chem.*, 2014, ***753*,** 27.

18 H. He, A. Gurung and L. Si, *Chem. Commun.*, 2012, **48**, 5910.

19 J. Bisquert and V. S. Vikhrenko, *J. Phys. Chem. B*, 2004, **108**, 2313.